Evolutionarily Optimal Phage Life-History Traits: Burst Size *vs.* Lysis Time

Joan Roughgarden
Hawaii Institute of Marine Biology, University of Hawaii
Department of Biology, Stanford University

January 30, 2026

Abstract

A dynamical equation for the virus to microbe ratio (VMR) during log phase population growth shows that an optimal balance occurs between a short lysis time with low burst size *vs.* a long lysis time with large burst size. The model predicts that interventions lowering phage adsorption by killing free virus and/or limiting their access to bacteria favors the evolution of an increased lysis time and higher burst per infecting microbe until the intervention either drives a virulent phage extinct or, for temperate phage, drives the phage from its lytic phase into its lysogenic phase. The model also predicts that along an environmental gradient of increasing primary productivity the optimal lysis time shortens along the gradient, implying that the lytic life cycle goes around faster along the gradient. However, the virion productivity realized during the time step corresponding to each point along the primary-productivity gradient remains constant.

Introduction

Breitbart (2012) noted that "It is difficult to find a paper in marine viral ecology that does not begin with a statement about the sheer abundance of viruses". The same is true today. Even though abundance estimates for virus have been available for over twenty years, the magnitude still seems incomprehensible. The number of prokaryotes on earth is 4–6 x 10^{30} cells with a production rate of 1.7 x 10^{30} cells/yr (Whitman *et al*. 1998). The number of virus is about ten times the number of prokaryotes (Wommack and Colwell 2000) implying that the number of virus is on the order of 10^{31}. In comparison, the number of grains of sand on all the earth's beaches is only 4 x 10^{20} and the number of stars in the universe a meager 2 x 10^{19} (Plait 2025).

Moreover, marine phage infect approximately 10^{23} bacteria every second, removing 20%–40% of the standing stock of marine bacteria each day (Suttle 2007). They exert top-down control of marine microbial abundance comparable to that of zooplankton grazing (Breitbart *et al.* 2018). Reports of viral abundance also appear for soil (Srinivasiah *et al*. 2008, Williamson *et al*. 2017) and the human gut (Townsend *et al*. 2021, the "phageome"). A synthetic review appears in (Brown *et al*. 2022).

Furthermore, virus are ancient with differences so great among them that the taxonomic rank of "realm" has been coined to reside at atop 15 lower ranks that include multiple kingdoms as well as the taxa below that (ICTV 2020, Koonin *et al.* 2020, 2021, Harris and Hill 2021). Marine phage represent 94% of the nucleic-acid-containing particles in the oceans (Breitbart *et al.* 2018). Hence, phage represent an enormous number of evolutionary agents whose phenotypes are shaped by natural selection.

What then are the phage phenotypes that natural selection is shaping? Of the many traits phage possess, including their morphology and mechanisms of inheritance and replication, the life-history

traits of the lytic/lysogeny switch, the burst size and the latency period are of particular interest because these traits underly the reproductive rate of phages. Ideally, research might offer an evolutionary explanation for such traits across various habitats. A previous paper introduces a model that predicts conditions for the lytic/lysogenic switch to occur and compares the model's predictions with ecogeographic patterns of the ratio of lytic to lysogenic life cycles (Roughgarden 2024). However, information on possible ecogeographic patterns in burst size and latency across habitats is limited. Both traits vary considerably across and within habitats, often in accordance with transient environmental conditions such as temperature (Wommack and Colwell 2000, Weinbauer 2004, Greenrod *et al.* 2024). Parada *et al.* (2006) show a correlation between burst size and bacterial productivity in coastal waters, but do not present data on latency times. Ranasinghe (2019) offers an extended review of burst size and latency across various categories of virus, but does not report the habitats where the virus live. This article extends the model in (Roughgarden 2024) to explain burst size and latency and predicts possible ecogeographic patterns whose discovery would test the model.

Interventions to control microbes with antibiotics have produced antibiotic resistance (Martinez *et al.* 2008, Davies and Davies 2010). These and other interventions might affect virus as well. The model in this article also predicts the evolutionary consequences for phage of interventions that lower the overall adsorption rate by virus onto bacteria.

This article explains burst size and latency as an evolutionarily optimal balance between reproducing early to benefit from geometric growth versus reproducing late to benefit from the time to produce a large burst size. The study of an evolutionary tradeoff between the benefits of early and late lysis time enjoys a long history (Abedon 1989, Wang *et al*. 1996, Abedon *et al*. 2001, Abedon *et al*. 2003, Bull *et al*. 2004, Bull 2006, Bull *et al*. 2006, Wang 2006, Heineman and Bull 2007, Bull *et al*. 2011, and Kannoly *et al*. 2022). The models developed in that literature are based on systems of delay-differential equations with viral colonization represented as a mass action term, that is, as $(V \times B)$ to represent collisions of virus with bacteria, and also feature density dependence in the bacteria population growth. The analysis of these equations generally involves solving for the equilibrium abundance of uninfected bacteria, infected bacteria and free phage.

This article differs from the preceding literature in being based on a new model that is defined in discrete time and features viral colonization of bacteria as a Poisson process. The model pertains to a virus-bacteria system in the log phase, where both populations grow exponentially rather than exist at equilibrium. The model anticipates a bust-boom environment where bacteria frequently experience exponential growth rather than a stable environment where an equilibrium can be attained. The model's analysis rests on a single dynamical equation for the virus to microbe ratio (VMR) rather than a system of coupled equations. Thus, the situation in which the optimal life history evolves is envisioned differently here as compared to the earlier literature—log phase versus stationary phase, recursion equations in discrete time versus delay-differential equations in continuous time, and Poisson colonization versus mass action infection. The Discussion section features a more detailed comparison of the differing intuition behind the earlier models compared to the present model.

Two experimental studies (Wang 2006, Kannoly *et al*. 2022) demonstrate that an optimal balance between lysis time and burst size exists. Hence, the reality of an optimal balance can now be taken as established. Instead, this article concerns how to predict *what* that optimal balance is. In nature, phage may not always possess the optimal balance for their present circumstances, but knowing the optimal balance in those circumstances reveals the direction toward which evolutionary change will occur.

The article has five sections: The first defines the basic population-dynamic model. The second extends the model to predict the optimal lysis time and burst size. The third compares the predicted the optimal lysis time and burst size to data from experiments with λ-phage and *Escherichia coli* (Wang 2006). The fourth predicts the evolutionary impact of interventions that affect the adsorption rate. The fifth develops predictions for ecogeographic patterns in lysis time and burst size.

Model

Population Dynamics of Phage and Bacteria

The phage/bacteria population-dynamic model is defined in discrete time with the time step being the viral lysis time period (Roughgarden 2024). A time step begins with the state variables, $N(t)$ and $V(t)$ for the number of bacteria and free virus particles (virions), respectively, in their environmental source pools at time t. Then the virus infect the bacteria with Poisson sampling such that some bacteria remain uninfected, some have only one infection, some have two infections *etc*. (Ellis and Delbrück 1939).

The Poisson distribution describing the infection process has density parameter, $\mu(t) \equiv a(v(t))\, v(t)$ where $v(t) \equiv V(t)/N(t)$ is the ratio of virus to bacteria in their source pools (the environmental virus to microbe ratio, VMR). The $a(v(t))$ is the adsorption function—it refers to the process whereby a viral particle comes in contact with a bacterium, binds to surface molecules, and then is incorporated into the bacterial cell. Adsorption is a function of $v(t)$ because the number binding sites on the surface of the bacterium is finite and the sites may become saturated.

With a Poisson distribution, μ is the average total adsorption per time step for a given v. Upon measuring μ, the adsorption coefficient is calculated as $a = \mu/v$ for the given v. Repetition for several values of v yields several values of μ from which the corresponding values of a are calculated. The values of a are then fitted to a curve yielding the adsorption function, $a(v)$.

According to a Poisson density function, the fraction of bacteria that remain uninfected, $P_0(\mu(t))$, is $e^{-\mu(t)}$ and the fraction of bacteria colonized by m virus, $P_m(\mu(t))$, is $\frac{e^{-\mu(t)}\mu(t)^m}{m!}$ for $m \geq 0$. The m indexes the number of virus per bacterium, called the multiplicity of infection (MOI). The fraction of bacteria that are infected by one or more virus is $1 - P_0(\mu(t))$.

The uninfected bacterial population increases by a geometric factor of increase per time step, R. If $R > 1$, the bacteria can increase in the absence of the virus. Accordingly, the uninfected bacteria resupply the bacterial source pool as

$$N(t+1) = R\, P_0(\mu(t))\, N(t). \tag{1}$$

Thus, the population size of bacteria at time $t+1$ equals R times the number of bacteria that are not infected. The R refers to microbial population growth over the time step.

Meanwhile, the virus within the infected bacteria produce new virus particles as

$$V(t+1) = \Big(b(1)\, P_1(\mu(t)) + b(2) P_2(\mu(t)) + \dots \Big)\, N(t), \tag{2}$$

where $b(m)$ is the burst size from a bacterium infected with m virus particles. Thus, the population size of virions at time $t+1$ equals the number of virions produced from bacteria infected by one phage, plus those produced from bacteria infected by two phage, plus those from bacteria infected with three phage, and so forth. No unadsorbed phage carry over to the next time step—they are lost. The phage at each time step are newly produced as bursts from infected bacteria. Together, Eqs. 1 and 2 constitute a dynamical system consisting of coupled recursion equations for bacteria and phage.

The envisioned scenario is that temperate virus in the infected hosts either lysogenize as prophages or burst out into the media where they colonize empty hosts, and then the cycle repeats. The burst of virions is analogized to pollen. Oak trees fill the air with trillions of pollen grains some of which adsorb to stigma and the rest disappear. The next year the cycle repeats. Similarly, barnacles release trillions of larvae into the water column. Some return to colonize empty rocks while the rest are lost. And phage in marine plankton can burst and infect other bacteria or disappear.

The viral adsorption is assumed to depend on the virus to microbe ratio, v,

$$a(v(t)) = a_o\,(1 - \frac{v(t)}{\kappa}), \tag{3}$$

where κ is the saturation coefficient—the virus to microbe ratio at which all the binding sites per bacterium are occupied and a_o is the maximum adsorption coefficient that occurs when all the binding sites are available.

To illustrate how to measure the adsorption function, suppose a vessel of known volume is provided with 10,000 phage and 100 bacteria—this corresponds to $v = 100$. After a time step, determine how many phage are left. Say, the number phage left in one replicate is 9,990 indicating that 10 phage were adsorbed. In two more replicates, the adsorbed number was 12 and 8, respectively, so the average is 10 adsorbed—this is μ for $v = 100$. Therefore, $a(100) = \mu/v = 10/100 = 0.10$. Suppose further that this experiment is repeated for various v. If the vessel is provided with 20,000 phage and 100 bacteria, corresponding to $v = 200$, then say, 14 are adsorbed on average. Therefore, $a(200) = 14/200 = 0.07$. Continuing, with 30,000 phage and 100 bacteria, $v = 300$, the number adsorbed turns out to be 15 on average so that $a(300) = 15/300 = 0.05$. Thus, total adsorption, μ, increases with v, while the adsorption per unit VMR, a, decreases with v as the receptor sites fill up. The best fit of a line to the points, (100, 0.10), (200, 0.07), (300, 0.05), is $a(v) = 0.12333 - 0.00025\,v$. The Y-intercept of the line is $a_o = 0.12333$, the maximum adsorption coefficient pertaining to the limit, $v \to 0$. The X-intercept of the line is $\kappa = 493.33$, the value of v for which the adsorption coefficient is zero, reflecting saturation of all the bacterial receptor sites. Except for the section comparing the model's predictions with experimental results, the adsorption coefficient is interpreted qualitatively.

For a finite vessel, the density of the microbes (N/volume) is implicit in the value measured for a_o. For a given N, virus in a small vessel with a high density of bacteria have a higher adsorption rate than virus in a large vessel with low microbial density because more virus to bacteria contacts occur in the small vessel than the large vessel during the time step. If N increases through time in a finite vessel, the density increases making the absorption parameter, a_o, also increase through time. In an open infinite environment however, the local microbial density may remain relatively constant as the microbial population spreads through space so that a_o may remain relatively constant. A strong dependence of a_o on N would represent a source of nonlinear feedback that may affect the phage-bacteria population dynamics. The analysis of this awaits a future paper. In addition to N and vessel size, a_o also depends on myriad other local environmental conditions such as media viscosity, convection currents in the media from micro turbulence in the ocean or stirring in a laboratory beaker, air fans and filters, strength of the virus to bacterial binding, and temperature. Many micro processes underly the realized adsorption. The μ is the bottom line, so to speak—the total adsorption per time step in the local conditions integrated over all the local micro processes that bring about the adsorption. Then the a_o is the total adsorption divided by the virus to microbe ratio responsible for the adsorption.

Turning now to burst size, several choices are available for a bacterium as a function of the number of virus in it, $b(m)$. The burst size might increase linearly with m so that $b(m) = b_o\,m$ where b_o is the contribution to the overall burst made by a single viral particle (Patel and Rao 1984, Figures 1–2). This case pertains to the absence of density dependence in burst size. Another possibility is where $b(m)$ to be a concave increasing function of m (Gadagkar and Gopinathan 1980, Figures 4–5). In this case, the burst-size function might be taken as $b(m) = b_o\,m^{\alpha}$ where α is an exponent between 0 and 1, say 1/2. This case shows limited density dependence in burst size. Still a third possibility is that $b(m)$ is a constant, $b(m) = b_o$, indicating strong density dependence. This situation is described in Ellis and Delbrück (1939) who write, "The bacteria which had adsorbed several phage particles behaved as if only one of these particles was effective." This case postulates that one infection disables all subsequent infections so that the burst is exactly the same with $m = 1$ as it is for all $m > 1$, a claim of

uncertain plausibility. A final possibility is to allow α to be negative, say $\alpha = -1$, to indicate that burst size varies inversely with the multiplicity of infection, indicating extremely strong density dependence as a response to "superinfection" (Brown and Bidle 2014). All these relations between burst size and m may be subsumed by taking $b(m) = b_0\, m^{\alpha}$ with α as 1, 1/2, 0, or -1. The cases of $\alpha = 1$ and $\alpha = 0$ were presented in Roughgarden (2024) and results for other α were noted, but not shown.

Here, the burst size as a function of the multiplicity of infection is taken as

$$b(m) = b_o\, m, \tag{4}$$

where b_o is the burst per virus infecting the bacterium. Even if $b(m)$ is not linear throughout the range of possible m, the linear form can be viewed as a Taylor approximation in the limit as $m \to 0$. This approximation is appropriate because the subsequent analysis focusses on the conditions for the virus to increase when rare into a bacterial population that is growing in its log phase—in such a circumstance m is small.

With $a(v(t))$ from Eq. 3, the equation for $N(t+1)$ from Eq. 1, becomes explicitly

$$N(t+1) = R\, e^{-a(v(t))\, v(t)}\, N(t). \tag{5}$$

The sum in the equation for $V(t+1)$ from Eq. 2 can be found using properties of the Poisson distribution combined with $b(m)$ from Eq. 4, yielding

$$V(t+1) = b_o \left(\sum_{m=1}^{\infty} m\, P_m(\mu(t)) \right) N(t) = b_o\, \mu(t)\, N(t).$$

Because $\mu(t) = a(v(t))\, v(t)$, and $v(t) \equiv V(t)/N(t)$, the equation above becomes

$$V(t+1) = b_o\, \left(a(v(t))\, v(t)\right)\, N(t) = b_o\, \left(a(v(t))\, \frac{V(t)}{N(t)} \right)\, N(t),$$

which reduces to

$$V(t+1) = b_o\, a(v(t))\, V(t). \tag{6}$$

Both the equations for $N(t+1)$ and $V(t+1)$ involve the virus to microbe ratio, $v(t)$. The dynamical equation for their ratio is found by dividing Eq. 6 by Eq. 5 yielding

$$\frac{V(t+1}{N(t+1)} = \frac{b_o\, a(v(t))\, V(t)}{R\, e^{-a(v(t))\, v(t)}\, N(t)}.$$

Then identifying $\frac{V(t+1}{N(t+1)}$ with $v(t+1)$ and $\frac{V(t)}{N(t)}$ with $v(t)$ yields,

$$v(t+1) = \frac{b_o}{R}\, \frac{a(v(t))}{e^{-a(v(t))\, v(t)}}\, v(t). \tag{7}$$

Equation 7 is a dynamical equation in one variable, $v(t)$, identical to Eq. 8 in Roughgarden (2024). The $v(t)$ may approach a stable virus to microbe ratio, $\hat{v}$, at which both the virus and bacteria grow geometrically with the same factor each time step. Moreover, even if $\hat{v}$ exists and is stable, the virus-bacteria pair may nonetheless go extinct because, in Eq. 5, $R \times$ the factor, $e^{-a(\hat{v})\, \hat{v}}$, may be less than one, even though R is greater than 1. This factor, called the "infection discount" in Roughgarden (2024), indicates the degree to which the bacterial population growth factor is discounted as a result of the morality caused by viral infections. The infection discount is generally less than 1 but approaches 1 as $\hat{v}$ approaches 0, indicating that a low virus to microbe ratio has little effect on the net bacterial growth.

In contrast, a high virus to microbe ratio implies that many microbes are being infected and killed. This strongly discounts the intrinsic microbial geometric growth factor, R, so that the net geometric growth factor can be less than one even though the geometric growth factor for the uninfected microbes is greater than one.

Unlike Roughgarden (2024), this paper does not focus on the stable virus to microbe ratio, $\hat{v}$. Instead, the focus is on the condition for increase when rare for a virus, that is, the condition when a virus can invade and infect a population of microbes. What traits does a virus need, and specifically what lysis time and burst size does it need, to invade faster than other viruses with other lysis times and burst sizes?

So, in the limit, $v(t) \to 0$, the dynamical equation in Eq. 7, upon suppressing the subscripts, reduces to

$$v(t+1) = \frac{b\,a}{R} v(t). \tag{8}$$

The virus population can infect the bacterial population if it can increase when rare, *ie.*, if $v(t) \approx 0$, then $v(t+1) > v(t)$. Inspection of Eq. 8 shows that if

$$b\,a > R, \tag{9}$$

then the virus can spread into a population of increasing bacteria. Alternatively, for a virulent virus, if $b\,a/R < 1$, the virus goes extinct because the virus cannot keep up with bacterial population growth. But for a temperate virus, if $b\,a/R < 1$, the virus switches to a prophage because its population grows faster as part of the bacterial genome than by bursting new virions each time step. This criterion was introduced in Roughgarden (2024).

Optimal Balance Between Burst Size and Lysis Time

This section applies the phage-bacteria population-dynamic model of the previous section to the tradeoff between burst size and lysis time.

Wang (2006) experimentally determined a functional relation between burst per infecting virus and lysis time as

$$\begin{aligned} b &= \beta\,(l-\epsilon) \quad \text{for} \;\; l > \epsilon \\ &= 0 \quad \text{for} \;\; l \le \epsilon, \end{aligned} \tag{10}$$

where l is the lysis time, ϵ is the eclipse, which is the time needed for the viral replication to commence, and β is the phage production rate (also called the phage maturation rate) once viral production has begun. The burst per virus increases linearly with the lysis time period after the eclipse has transpired. (These symbols and all the others used in the paper are listed in Table 1.)

The geometric growth factor of uninfected microbes, R, in Eq. 1 refers to microbial population growth over a time step. Because the lysis time, and hence the time step, can vary it is useful to refer the geometric factor to units of a minute, rather than to the time step itself. Hence, define ρ as the uninfected microbe geometric growth factor per minute. Then the growth factor for a time step of length, l, is

$$R = \rho^{l} \tag{11}$$

Because the time step in the model, Eq. 8, is the lysis time, l, to investigate how the time step itself evolves, a maximum time step, L, is stipulated that is longer than the largest feasible lysis time. Then the dynamical equation is iterated for the number of l that fit within L, given the eclipse. For example, suppose the eclipse is 0 and L is 100. If l is also 100, then only one iteration takes place within L,

whereas if l is 1, then 100 iterations fit within L, and if l is 25, then four iterations fit within L, and so forth. Thus, for a given l, the v after the number of iterations that fit within L is

$$v(t+L) = \frac{(\beta\ (l-\epsilon)\ a)^{\lfloor \frac{L}{l} \rfloor}}{(\rho^l)^{\lfloor \frac{L}{l} \rfloor}}\, v(t), \tag{12}$$

for l = (ϵ+1, ϵ+2 ... L) where $\lfloor \frac{L}{l} \rfloor$ indicates the integer part of $\frac{L}{l}$. This is the number of iterations of viral reproduction with lysis time, l, that fit into L.

The numerator of Eq. 12 is the production of virions from a lytic virus over the number of time steps of size, l, that fit into the interval, L.

The denominator of Eq. 12 is the bacterial production over the number of time steps of size, l, that fit into the interval, L. This is also the production of a temperate virus residing as a prophage in the bacterial chromosome. The geometric growth factor for a microbe over a single time step of length l is ρ^l. The l in the exponents within the denominator cancel leaving, $l \times \frac{L}{l} = L$.

Further analysis is aided by taking a continuous approximation in Eq. 12, as though a fractional iteration can fit into L,

$$v(t+L) = \left(\frac{(\beta\ (l-\epsilon)\ a)^{\frac{L}{l}}}{\rho^L} \right)\, v(t), \tag{13}$$

for $l > \epsilon$. The expression in large parentheses in Eq. 12 is the relative fitness of a lytic phage relative to the prophage residing in the bacteria over the period, L, as a function of l,

$$W_L(l) = \frac{(\beta\ (l-\epsilon)\ a)^{\frac{L}{l}}}{\rho^L}. \tag{14}$$

The optimal lysis time, $\hat{l}$, is found by maximizing $W_L(l)$ with respect to l. The corresponding optimal burst per infecting microbe, $\hat{b}$, is found from Eq. 8, evaluated at $l = \hat{l}$.

To find the optimal lysis time, differentiate W_L with respect to l, yielding

$$\frac{d\,W_L(l)}{d\,l} = \frac{(\beta(l-\epsilon)a)^{\frac{L}{l}}}{\rho^L}\ \frac{L}{l}\ \left(\frac{1}{(l-\epsilon)} - \frac{\log\left(\beta\,(l-\epsilon)\ a\right)}{l} \right).$$

This equation contains the expression in large parentheses defined as

$$Y(l) = \frac{1}{(l-\epsilon)} - \frac{\log\left(\beta\,(l-\epsilon)\ a\right)}{l}. \tag{15}$$

The root, $Y(l) = 0$, of this expression is the optimal lysis time, $\hat{l}$. The $Y(l)$ is independent of both L and ρ, and therefore, so is $\hat{l}$.

The critical lysis time, $l_c(L)$, at which being lytic becomes a better strategy than being a prophage over the period, L, is found by setting

$$W_L(l) = 1, \tag{16}$$

and solving for l. If the optimal lysis time, $\hat{l}$, is less than $l_c(L)$, the virus is better off not lysing at all during the period, L, and instead incorporating as a prophage into the bacterial chromosome. Alternatively, if $\hat{l}$, is greater than $l_c(L)$, the virus is better off infecting and lysing the bacteria during the period, L, while doing so with the optimal lysis time. The optimal lysis time produces a corresponding optimal burst per infecting virus found from Eq. 10 evaluated at $l = \hat{l}$.

Table 1: Symbols

Symbol	Description	Units
V	Number free virus particles (virions)	Organisms
N	Number of microbes (bacteria)	Organisms
v	Virus to microbe ratio, VMR,	None
R	Geometric factor of increase per time step for microbes	None
ρ	Geometric factor of increase per minute for microbes	None
μ	Poisson density, average total adsorption per time step	Organisms
$P_m(\mu)$	Probability microbe colonized by m virus	None
$a(v)$	Adsorption function, total adsorption per VMR	Organisms
a_o	Maximal total adsorption per VMR when VMR is low	Organisms
κ	Saturation VMR	None
$b(m)$	Burst per microbe as function of multiplicity of infection	Organisms
b_o	Burst per infecting virus	Organisms
a	a_o with subscript suppressed	Organisms
b	b_o with subscript suppressed	Organisms
l	Lysis time (latency), same as time step	Minutes
L	Large time interval to include multiple time steps	Minutes
ϵ	Eclipse period, time before virus production starts	Minutes
β	Virus production rate once eclipse expires	Organisms per minute
W_L	Relative fitness of lytic to lysogenic phage over interval L	None
$Y(l)$	Expression whose root is optimal lysis time	None
$\hat{l}$	Optimal lysis time	Minutes
$\hat{b}$	Burst per infecting virus with optimal lysis time	Organisms
$l_c(L)$	Critical lysis time for lytic = lysogenic fitness over interval L,	Minutes
W_{Lo}	W_L assuming ϵ is zero	None
$\hat{l_o}$	Optimal lysis time assuming ϵ is zero	Minutes
$\hat{b_o}$	Optimal burst size assuming ϵ is zero	Organisms
$\widehat{W_{Lo}}$	Optimal W_L assuming ϵ is zero	None

Predictions

Comparison of Model with Laboratory Data

Table 2 gives the parameters for an illustration. The β and ϵ in units of phage/min and min, respectively, are derived from isogenic λ-phages with different lysis times from Wang (2006). The bacterial geometric factor of increase, R, from Wang (2006) for *Escherichia coli* K-12, is given as 2.04/hr—this converts to the value of ρ in the table in minutes. In the absence of an experiment to measure the adsorption parameter, a, a nominal value of 0.1 is used corresponding to the worked example provided earlier. The adsorption parameter varies considerably depending on environmental conditions affecting the accessibility of the bacteria to the virus and the number of binding sites per bacterium varies with nutrient conditions (Schwartz 1976, Philipson 1983). The large time interval, L, is taken arbitrarily as 100 minutes, a value comfortably larger than the optimal lysis time.

Table 2: Parameters

Name	Value	Notes
β	7.7	Wang 2006
ϵ	28	Wang 2006
ρ	1.035	$e^{2.04/60}$, Wang 2006
a	0.1	Nominal value
L	100	Large time interval

To find the optimal lysis time, using the NSolve[] function in Mathematica with $Y(l)$ in Eq. 15, together with the parameters from Table 2, returns the value,

$$\hat{l} = 45.5. \tag{17}$$

independent of L and ρ. The corresponding optimal burst per infecting virus from Eq. 10 is

$$\hat{b} = 134.7. \tag{18}$$

and the corresponding maximal relative fitness over 100 minutes from Eq. 14 is

$$\widehat{W_{100}} = 9.7. \tag{19}$$

and the critical lysis time at which being lytic becomes a better strategy than being a prophage over 100 minutes works out to be

$$l_c(100) = 31.9. \tag{20}$$

Figure 1 shows the fitness of a lytic phage relative to a prophage after a period of 100 minutes as a function of the lysis time, l, based on the parameters in Table 2. Relative lytic to prophage fitness of 1 is shown as horizontal line. If l is greater than 31.9, then the lytic phase has a higher fitness than the lysogenic phase during the 100 minute interval. If l is between ϵ and $l_c(100)$, *i.e.* between 28 and 31.9 minutes, then the phage cannot coexist during the interval with the bacteria in its lytic phase—the bacteria population grows faster than the viral population, leaving it behind, so to speak. Instead, the phage must lysogenize—incorporate into the bacterial genome to acquire the population growth rate of the bacteria.

Wang (2006) measured the fitness of 11 strains of λ-phage whose latencies varied from 28.3 to 63.0 minutes. The study found that the strain whose lysis time was 51.0 minutes had the highest fitness, a value quite close to that predicted in the model here, 45.5, based on the parameters in Table 2. The burst per infecting virus for the strain with the highest fitness was 170.0, also fairly close to the value predicted here, 134.7. This initial degree of agreement between theory and experiment is coincidental because the nominal value of the adsorption parameter, a, in Table 2 was not experimentally determined.

Instead, suppose a is lowered to 0.052. Then $\hat{l}$ works out to be 50.0 and $\hat{b}$ to 176.9, almost exactly the same as Wang(2006) found experimentally. Thus, lowering a from the nominal value of 0.100 to 0.052, while keeping the other parameters from Table 2 the same, brings the predicted optimal lysis time and burst per infecting virus into close agreement with the experimental results. The next section considers further implications of variation in a.

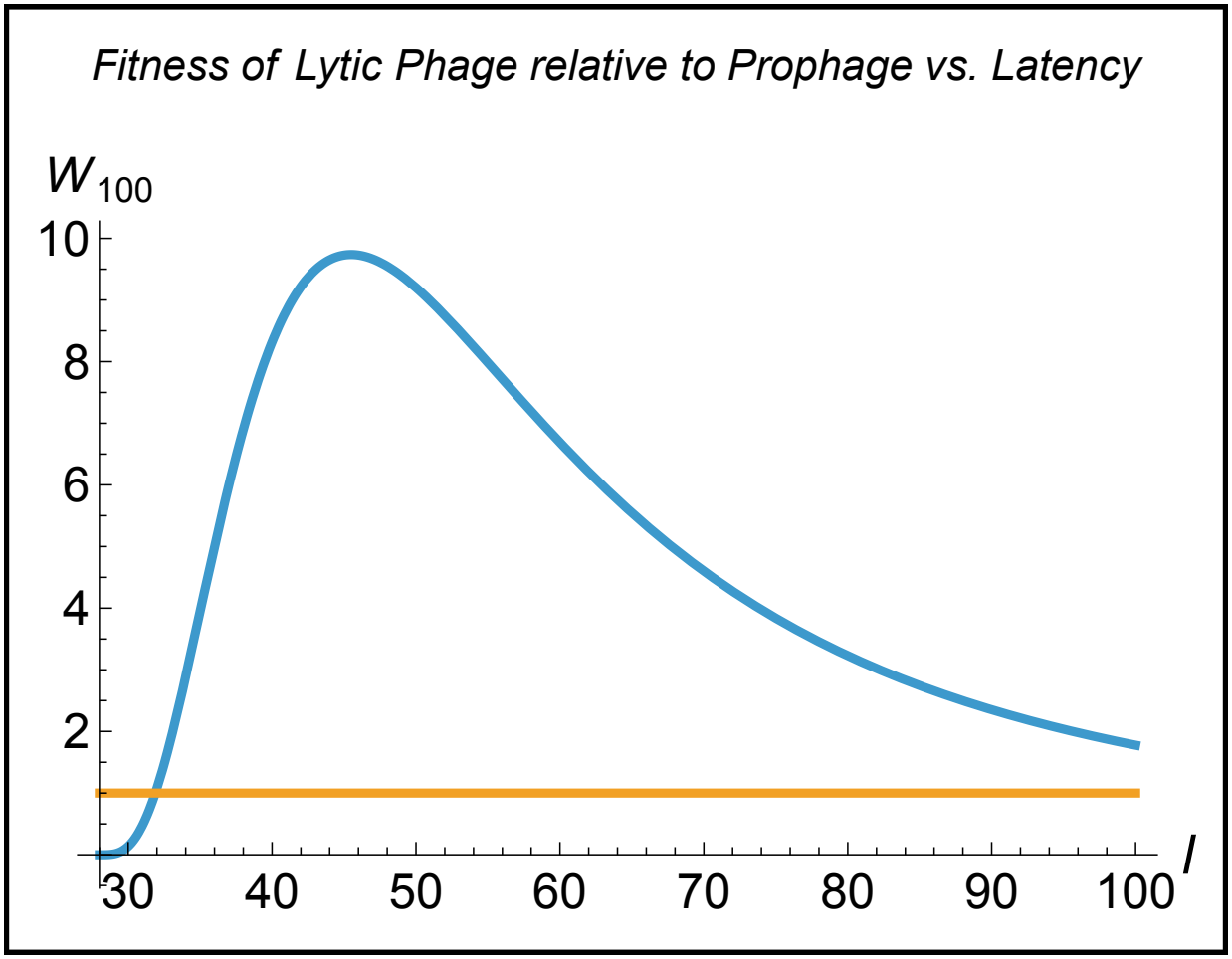

Figure 1: *Fitness of lytic phage relative to prophage after 100 minutes, W_{100}, as a function of the lysis time, l, is a humped-shaped curve starting from the eclipse period of 28 minutes. The optimal lysis time occurs at $\hat{l}$ = 45.5 which yields a maximum ratio of lytic to prophage fitness, $\widehat{W_{100}}$, of 9.7 over the 100 minute interval. Relative lytic to prophage fitness of 1 is shown as horizontal line. The hump-shaped curve for W_{100} intersects the line at $l_c(100) = 31.9$. Thus, the fitness of a lytic phage exceeds that of a prophage during the 100 minute interval when the lysis time exceeds 31.9. If the lysis time of the phage is between 28 and 31.9, the phage cannot coexist with the bacteria during the 100 minute interval unless it becomes a prophage.*

Interventions that Impact Adsorption

Figure 2 shows the impact of varying adsorption on phage evolution. The figure starts with a at a low value for which the phage exists as a prophage. Then increasing a induces the phage to excise from the bacterial chromosome when the ratio of lytic to prophage fitness equals 1. Thereafter, as a increases even more, the optimal latency and bust size progressively decrease while the relative fitness of the lytic to prophage progressively rises.

Many interventions to control phages, and viruses more generally, involve techniques such as air or water filters, or controlling humidity that lower the adsorption of phage by bacteria (*cf.* Sobsey *et al.* 2008, Clokie and Kropinski 2009, Wommack *et al.* 2009, Moriyama *et al.* 2020, Curtius *et al.* 2021, Van Charante *et al.* 2021, Beltrán *et al.* 2023). Overall, the model predicts that interventions lowering a cause the evolution of an increased lysis time and correspondingly higher burst size until the intervention is sufficient either to drive a virulent phage extinct, or for temperate phage, to drive the

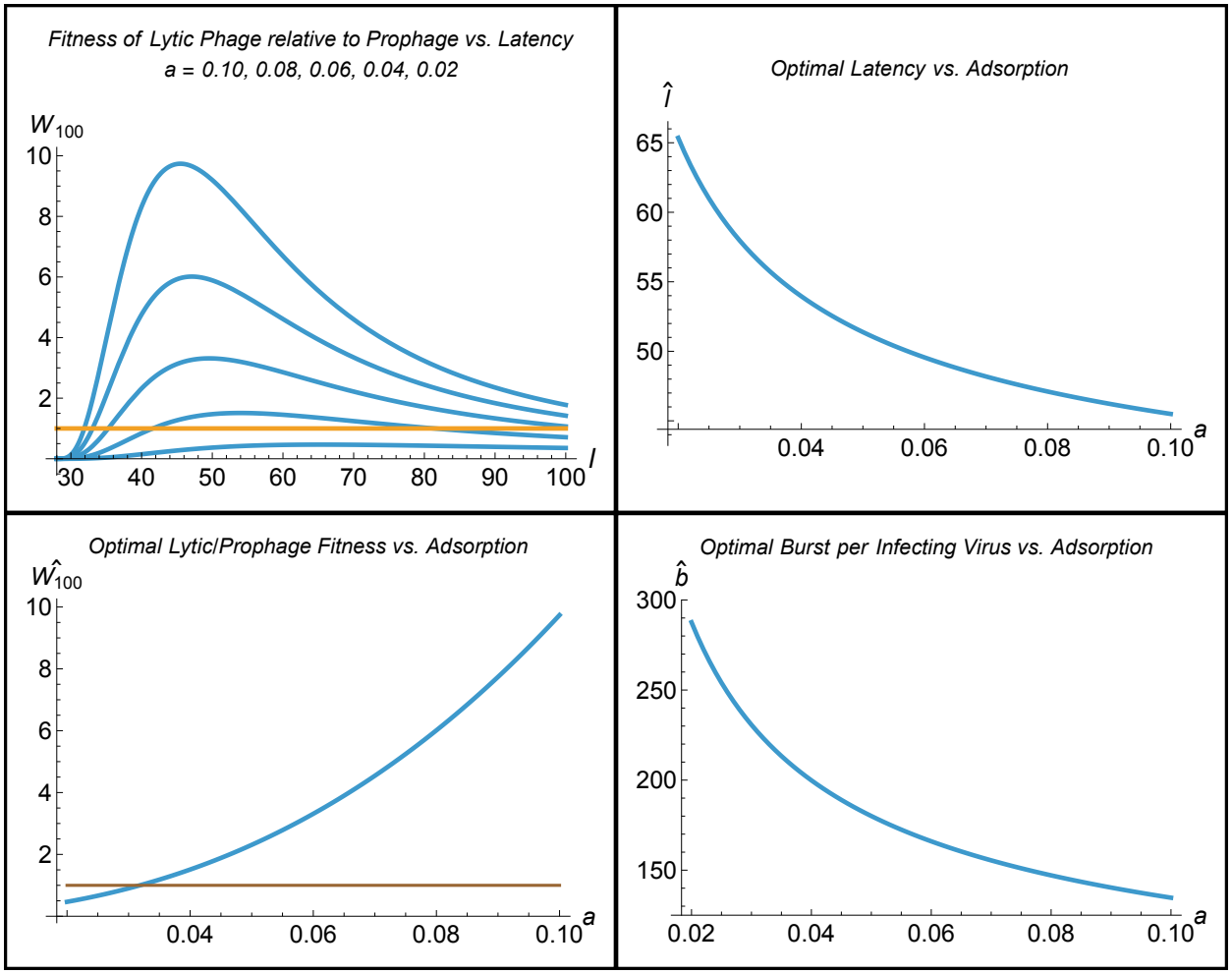

Figure 2: *Impact of varying adsorption on phage evolution. Top left: Fitness of the lytic phase* vs. *lysis time for several values of the adsorption coefficient,* a*. The top curve is for* a *= 0.10 and is identical to that shown in Figure 1. The curves below the top are successively for* a *= 0.08, 0.06, 0.04, and 0.02. The horizontal line is a relative fitness of 1 where the fitness of a lytic phage equals that of a prophage. As* a *decreases, the peaks of the curves for the lytic phase progressively become lower and shift to the right. Top right: Optimal lysis time* vs. *the adsorption parameter,* a*. As* a *increases from 0 to 0.10, the optimal lysis time decreases. Bottom right: Optimal burst per infecting virus* vs. *the adsorption parameter,* a*. As* a *increases from 0 to 0.10, the optimal burst size also decreases, reflecting the decreasing lysis time. Bottom left: Optimal fitness of a lytic phage relative to the prophage* vs. *the adsorption parameter,* a*. The horizontal line is a relative fitness of 1 where the fitness of a lytic phage equals that of a prophage. As* a *increases from 0 to 0.10, the optimal lytic/prophage fitness ratio starts below 1 and increases, intersecting the horizontal line at* a *= 0.032, at which point the prophage becomes induced to excise from the bacterial chromosome and become lytic.*

phage from its lytic phase into its lysogenic phase.

Ecogeographic Patterns

Prevalence of the lysogenic life cycle relative to the lytic life cycle increases in conditions that promote bacterial productivity. For example, overfishing and eutrophication on coral reefs causes an increase in ungrazed fleshy algae. These release dissolved organic carbon that promotes bacterial productivity, leading to a condition called microbialization. Knowles *et al.* (2016) and Silveira *et al.* 2021)

show that lysogeny increases with microbialization on coral reefs. Another example involves the guts of mammals. Here concentrated nutrients promote bacterial productivity, resulting in gut bacteria that are enriched with prophages, (López-Leal *et al.* 2022). Generally speaking, increasing bacterial productivity relative to virion productivity increases the likelihood of the lysogenic lifecycle relative to lytic lifecycle because reproduction as a prophage becomes better than reproduction through lysis (Roughgarden 2024).

Not as many ecogeographic patterns are known for burst size and latency time as for the lysogenic to lytic ratio. However, in one study, Parada *et al.* (2006, Fig. 5) showed a positive relationship between bacterial productivity and viral burst size in the North Sea. In terms of the model, high nutrient conditions increase both ρ, the bacterial geometric growth factor and perhaps β, the number of new virions produced per infecting virus per minute of latency. High nutrient conditions might affect also a, the absorption coefficient depending on whether high nutrients increase or decrease bacterial density.

The eclipse period may a quarter to a half of the overall latency, being about 10 minutes for the phage T7 whose latency is 40 minutes at $30°$ (Endy *et al.* 1997, Fig. 6) and 28 minutes for λ phage with an optimal latency of 51 minutes, as discussed earlier (Wang 2006, *cf.* Table 2). Still, qualitative insight might be gained by letting ϵ be zero. Accordingly, Eq. 14 becomes

$$W_{Lo}(l) = \frac{(\beta\ a\ l)^{\frac{L}{l}}}{\rho^L}. \tag{21}$$

By differentiating $W_{Lo}(l)$ with respect to l, setting the result equal to zero and solving for l, yields an explicit result for the optimal latency

$$\hat{l_o} = \frac{e}{\beta\ a}, \tag{22}$$

where e is Euler's Number, the base of the natural logarithms, and not the eclipse, ϵ. Thus, the optimal latency for the virus varies inversely with how good the environment is for the lytic phase. The more favorable the environment is for the lytic phase, $(\beta\ a)$, the shorter the optimal latency. That is, the better the environment is for the lytic phase, the faster the virus goes around its life cycle. Specifically, Figure 3 (Left) shows $\hat{l_o}$ as a function of $(\beta\ a)$ from Eq. 22.

The burst per infecting virus realized during the optimal latency, from Eq. 10 with $\epsilon = 0$, is

$$\hat{b_o} = \beta\ \hat{l_o} = \frac{e}{a}. \tag{23}$$

The optimal burst per infecting virus is independent of β. To see why, suppose productive environmental conditions increase the speed at which new virions are produced, β. This leads to a shorter optimal latency, $\hat{l_o}$. Then the higher speed of virion production times the shorter latency cancel out leaving the burst per infecting virus unchanged. However, the optimal burst per infecting virus does vary inversely with a. A lower bacterial density leading to a lower a causes a higher burst per infecting virus according to Eq. 23.

The Parada *et al.* (2006) observations in which both bacterial productivity and viral burst size increase together across various sites in the North Sea can be reconciled with this model if both (1) higher nutrients increase ρ, as was observed, and (2) higher nutrients also decrease bacterial density, thereby lowering a, which in turn leads to higher burst per infecting virus according to Eq. 23. Also according to Eq. 23, any effect of nutrients on β is irrelevant. This ecological situation is where high nutrients cause high productivity and turnover associated with a low standing crop of bacteria, as is characteristic of grazed ecosystems (*eg.* Odum and Barrett 2005).

The virion productivity per the time step equalling the optimal latency is invariant because $\hat{b_o}$ depends inversely on a, in Eq. 23. The a therefore cancels out in

$$\hat{b_o}\ a = (\frac{e}{a})\ a = e \tag{24}$$

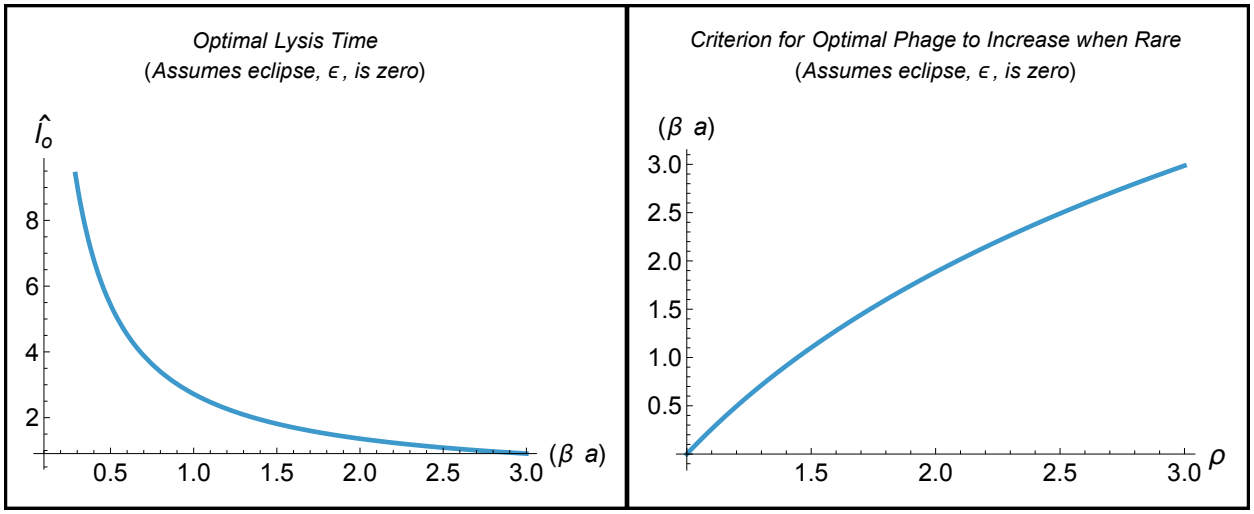

Figure 3: *Left: The optimal lysis time $\hat{l}_o$ as a function of the quantity $(\beta\, a)$, where β is the rate of virion production per minute of lysis time and a is the adsorption parameter, from Eq. 22. Right: Graph of criterion for increase when rare for an optimal lytic phage as a function of the bacterial geometric growth factor, ρ, from Eq. 27. If $(\beta\, a)$ is greater than the curve of $(e\, \log[\rho])$ then the virus can increase when rare, otherwise it is excluded from the system if virulent, or becomes lysogenic if temperate. If the lytic virus can increase when rare, the corresponding optimal lysis time can be read off the graph on the left.*

To see why, suppose the adsorption, a, increases. Then the optimal latency decreases. Therefore, the corresponding burst per infecting virus decreases too. The decreased burst per infecting virus then cancels out the increase in adsorption leaving the virion productivity per the time step corresponding to the optimal latency unchanged. So, as a and β are varied across environmental gradients, the optimal latency does vary according to Eq. 22. However, the virion productivity resulting from those varying latencies remains constant for the corresponding time steps.

The relative advantage of the lytic to lysogenic lifecycle can to be computed over a long period, L. Multiple iterations of the single-step model occur within this period that can be compared with bacterial population growth over the same period. The optimal virion productivity over L relative to the bacterial productivity over L is found by substituting Eq. 22 into Eq. 21 leading to

$$\widehat{W_{Lo}} = \frac{e^{\left(\frac{(\beta\, a)\, L}{e}\right)}}{\rho^L}. \tag{25}$$

The $\widehat{W_{Lo}}$ increases with $(\beta\, a)$ and decreases with ρ. To see the long-term relative advantage of the optimal lytic lifecycle to the lysogenic lifecycle, take the limit as L tends to infinity, yielding

$$\begin{aligned} \lim_{L\to\infty} \widehat{W_{Lo}} &= \infty \quad \text{if} \quad (\beta\, a) > e\, \log(\rho) \\ \lim_{L\to\infty} \widehat{W_{Lo}} &= 0 \quad \text{if} \quad (\beta\, a) < e\, \log(\rho). \end{aligned} \tag{26}$$

Thus, the optimal virus, *i.e.*, one with the optimal balance between latency and burst size, increases when rare over the long term if

$$(\beta\, a) > e\, \log(\rho), \tag{27}$$

otherwise it goes extinct or becomes lysogenic. That is, for an optimal virus, its productivity as a virion must exceed its productivity as a prophage to be virulent according to Eq. 27.

Figure 3 (Right) shows the criterion for increase when rare for an optimal lytic phage as a function of the bacterial growth factor, assuming the eclipse is zero, from Eq. 27. If $(\beta\, a)$ on the vertical axis is greater than the curve for $(e\, \log(\rho))$ then the virus can increase when rare, otherwise it is excluded from the system if virulent, or becomes lysogenic if temperate.

To pull these results together, consider a gradient in environmental factors along which the lytic productivity, $(\beta\, a)$, increases. Assume too that the eclipse, ϵ, is small. Then (1) the optimal lysis time shortens along the gradient, implying that the lytic life cycle goes around faster along the gradient, according to Eq. 22; (2) The burst per infecting virus does not vary along the gradient, according to Eq. 23, unless a changes because of bacterial density change along the gradient; and (3) the virion productivity realized during the time step corresponding to each point along the gradient remains constant, according to Eq. 24. If the bacterial productivity, ρ, also increases along this gradient, then the condition in Eq. 27 can flip. At the flipping point on the gradient, the virus either goes extinct or if temperate, switches to lysogeny.

Discussion

This article provides a mathematical model for the evolutionarily optimal balance between lysis time and burst size. Wang (2006) found the optimal lysis time with strains of λ-phage infecting *E. coli* to be 51 minutes. Kannoly *et al*. (2022) also measured strains of λ-phage infecting *E. coli* and found an optimal lysis time of 80 minutes. The value of the optimal lysis time differed between these studies because the environmental conditions in the experiments differed. Given the reality of an optimal lysis time that depends on environmental conditions, the issue is how to explain it.

This article explains the optimal lysis time by finding the optimal balance between rapid reproduction with a short lysis time at the cost of a low burst size *vs*. slow reproduction with a long lysis time and the benefit of a large burst size. The optimal balance between these two considerations is derived using a single dynamical equation in discrete time for the virus to microbe ratio (VMR) during the log phase of phage/bacteria population growth (Roughgarden 2024).

Previous models for the optimal balance use a system of delay-differential equations for the dynamics of uninfected bacteria, infected bacteria and free phage in the stationary phase of virus-bacterial population growth (*eg*. Bull 2006, Bull *et al*. 2006). The system of equations is an extension of the original delay-differential equation model introduced by Campbell (1961). The original Campbell model is critiqued in detail in Roughgarden (2024, incl. Supplementary Material).

In the present context, the relevant distinction between this paper and previous papers is the intuition behind the optimal lysis time. Eq. 4 in Bull (2006) gives a formula for the optimal lysis time, (called L). When the phage is at population-dynamic equilibrium (called $\hat{\lambda} = 0$) and when the eclipse (called E) is zero, then the optimal lysis time is $L = 1/d$, where d is the death rate of bacterial cells. This prediction from Eq. 4 in Bull (2006) for the optimal lysis time is completely different from Eq. 22 in this paper.

The intuition behind Eq. 4 of Bull (2006) for the optimal lysis time is that a high bacterial death rate implies a short life span for the bacteria, leaving only a short time for an infecting virus to make new virions. Thus, the tradeoff is between the time needed to produce a burst and the time available within a bacterial cell to do it. This explanation for the optimal tradeoff is conceptually different from that offered by this paper's model that focusses instead on the tradeoff between rapid reproduction with low burst *vs*. slow reproduction with high burst.

Another conceptual difference between Eq. 4 of Bull (2006) for the optimal lysis time *vs*. Eq. 22 here is that, colloquially speaking, in the former the virus is trying to synchronize its lysis time with the bacterial dynamics, whereas here, the virus is trying to find the best balance between early and late lysis irrespective of what the bacteria are doing. Then once the lytic virus is doing the best it can,

it compares what it achieves by remaining lytic with what it achieves by lysogenizing and decides to remain lytic or to switch to lysogeny according to which yields the higher fitness.

Grounds for preferring this paper's model over previous models, in addition to its simplicity and tractabilty, rest on which environmental situation is more common—log phase growth or stationary growth for the phage-bacteria pair. Previous models are directed to experimental situations such as a chemostat where a stationary phase can be realized. But in nature it is hard to imagine phage and bacteria in equilibrium. In nature the populations are invariably either recovering from or being decimated by environmental events such as storms *etc*. Natural populations of phage and bacteria are likely continually in a bust-boom regime where a log-phase model is preferable to a stationary-phase model.

The model of this paper predicts the evolutionary impact of interventions to control phage and predicts possible ecogeographic patterns of latency and burst size along environmental gradients. The model predicts that interventions lowering phage adsorption cause the evolution of an increased lysis time and correspondingly higher burst size until the intervention is sufficient either to drive a virulent phage extinct, or for temperate phage, to drive the phage from its lytic phase into its lysogenic phase. The model predicts that along a gradient in which the viral productivity increases, the optimal lysis time shortens and the lytic life cycle goes around faster.

All in all, this paper shows that the life-history traits of virus are not arbitrary, but vary in predictable ways associated with different environments.

Acknowledgments

The author thanks Cynthia Silveira of the University of Miami together with Forest Rohwer and members of the San Diego State University (SDSU) BioMath Group for discussion about this paper. The author also thanks the Editor, Jim Bull, and two anonymous reviewers for comments that greatly improved the manuscript. This article is Contribution #4 from a project, The Theory of Holobiont Evolution, funded by the Gordon and Betty Moore Foundation through Grant GBMF10000 to the University of Hawaii, J. Roughgarden, PI.

References

Abedon, S.T., 1989. Selection for bacteriophage latent period length by bacterial density: a theoretical examination. Microbial ecology, 18, pp.79–88.

Abedon, S.T., Herschler, T.D. and Stopar, D., 2001. Bacteriophage latent-period evolution as a response to resource availability. Applied and environmental microbiology, 67(9), pp.4233–4241.

Abedon, S.T., Hyman, P. and Thomas, C., 2003. Experimental examination of bacteriophage latent-period evolution as a response to bacterial availability. Applied and environmental microbiology, 69(12), pp.7499–7506.

Beltrán, E.O., Castellanos, J.E., Corredor, Z.L., Morgado, W., Zarta, O.L., Corté,A., Avila, V., Martignon, S,. 2023. Tracing ΦX174 bacteriophage spreading during aerosol-generating procedures in a dental clinic. *Clinical Oral Investigations* 27, 3221–3231 (2023). https://doi.org/10.1007/s00784-023-04937-z

Breitbart, M. 2012. Marine viruses: truth or dare. Annual review of marine science, 4:425–448.

Breitbart M, Bonnain C, Malki K, Sawaya N 2018. Phage puppet masters of the marine microbial realm. Nat Microbiol 3:754–66.

Brown, Christopher M. and Kay D. Bidle. 2014. Attenuation of virus production at high multiplicities of infection in Aureococcus anophagefferens. Virology 466-467 (2014) 71–81.

Brown, T.L., Charity, O.J. and Adriaenssens, E.M., 2022. Ecological and functional roles of bacteriophages in contrasting environments: marine, terrestrial and human gut. Current Opinion in Microbiology, 70, p.102229.

Bull, J.J., 2006. Optimality models of phage life history and parallels in disease evolution. Journal of theoretical biology, 241(4), pp.928–938.

Bull, J.J., Pfennig, D.W. and Wang, N., 2004. Genetic details, optimization and phage life histories. Trends in ecology & evolution, 19(2), pp.76–82.

Bull, J.J., Millstein, J., Orcutt, J. and Wichman, H.A., 2006. Evolutionary feedback mediated through population density, illustrated with viruses in chemostats. The American Naturalist, 167(2), pp.E39–E51.

Bull, J.J., Heineman, R.H. and Wilke, C.O., 2011. The phenotype-fitness map in experimental evolution of phages. PLoS One, 6(11), p.e27796.

Campbell, Allan. 1961. Conditions for the Existence of Bacteriophage. *Evolution* 15:153–165.

Chow, C. E. T., and Suttle, C. A. 2015. Biogeography of viruses in the sea. Annual review of virology, 2(1):41–66.

Clokie, Martha R.J. and Andrew M. Kropinski 2009 Bacteriophages Methods and Protocols, Volume 1: Isolation, Characterization, and Interactions. Humana Press

Curtius, J., Granzin, M. and Schrod, J., 2021. Testing mobile air purifiers in a school classroom: Reducing the airborne transmission risk for SARS-CoV-2. Aerosol Science and Technology, 55(5), pp.586-599.

Davies, J., and Davies, D. 2010. Origins and evolution of antibiotic resistance. Microbiology and molecular biology reviews, 74(3):417–433.

Ellis, E., and M. Delbrück. 1939. The growth of bacteriophage. *Journal of General Physiology* 22:365–384, doi: 10.1085/jgp.22.3.365.

Endy, D., Kong, D. and Yin, J., 1997. Intracellular kinetics of a growing virus: a genetically structured simulation for bacteriophage T7. Biotechnology and Bioengineering, 55(2), pp.375–389.

Gadagkar, R., and Gopinathan, K. P. 1980 Bacteriophage Burst Size during Multiple Infections, Journal of Biosciences, 2:253–9.

Greenrod, S. T., Cazares, D., Johnson, S., Hector, T. E., Stevens, E. J., MacLean, R. C., and King, K. C. 2024. Warming alters life-history traits and competition in a phage community. Applied and Environmental Microbiology, 90(5):e00286-24.

Harris, H. M., and Hill, C. 2021. A place for viruses on the tree of life. Frontiers in Microbiology, 11, 604048.

Heineman, R.H. and Bull, J.J., 2007. Testing optimality with experimental evolution: lysis time in a bacteriophage. Evolution, 61(7), pp.1695–1709.

ICTV (International Committee on Taxonomy of Viruses). 2020. The new scope of virus taxonomy: partitioning the virosphere into 15 hierarchical ranks. Nature Microbiology 5(5):668–674.

Kannoly, S., Singh, A. and Dennehy, J.J., 2022. An optimal lysis time maximizes bacteriophage fitness in quasi-continuous culture. MBio, 13(3), pp.e03593–21.

Knowles, B., C. B. Silveira, B. A. Bailey, K. Barott, V. A. Cantu, A. G. Cobián-Güemes, F. H. Coutinho, E. A. Dinsdale, B. Felts, K. A. Furby, E. E. George, K. T. Green, G. B. Gregoracci, A. F. Haas, J. M. Haggerty, E. R. Hester, N. Hisakawa, L. W. Kelly, Y. W. Lim, M. Little, A. Luque, T. McDole-Somera, K. McNair, L. S. de Oliveira, S. D. Quistad, N. L. Robinett, E. Sala, P. Salamon, S. E. Sanchez, S. Sandin, G. G. Z. Silva, J. Smith, C. Sullivan, C. Thompson, M. J. A. Vermeij, M. Youle, C. Young, B. Zgliczynski, R. Brainard, R. A. Edwards, J. Nulton, F. Thompson & F. Rohwer 2016. Lytic to temperate switching of viral communities. Nature 531: 466–470

Koonin, E. V., Dolja, V. V., Krupovic, M., Varsani, A., Wolf, Y. I., Yutin, N., ... and Kuhn, J. H. 2020. Global organization and proposed megataxonomy of the virus world. Microbiology and molecular biology reviews, 84(2):10-1128.

Koonin, E. V., Krupovic, M., and Agol, V. I. 2021. The Baltimore classification of viruses 50 years later: how does it stand in the light of virus evolution?. Microbiology and Molecular Biology Reviews, 85(3)10–1128.

López-Leal, Gamaliel, Laura Carolina Camelo-Valera, Juan Manuel Hurtado-Ramírez, Jérôme Verleyen, Santiago Castillo-Ramírez, Alejandro Reyes-Muñoza 2022. Mining of Thousands of Prokaryotic Genomes Reveals High Abundance of Prophages with a Strictly Narrow Host Range. mSystems 7:4 10.1128/msystems.00326-22.

Martinez, J. L., Fajardo, A., Garmendia, L., Hernandez, A., Linares, J. F., Martínez-Solano, L., and Sánchez, M. B. 2008. A global view of antibiotic resistance. FEMS microbiology reviews, 33(1):44–65

Moriyama, M., Hugentobler, W.J. and Iwasaki, A., 2020. Seasonality of respiratory viral infections. Annual review of virology, 7(1), pp.83–101.

Odum, E.P. and Barrett, G.W., 2005. Fundamentals of ecology Fifth Edition. Belmont: CA: Thomson Brooks/Cole.

Patel, I. R., and Rao, K. K. 1984 Bacteriophage Burst Size as a Function of Multiplicity of Infection, Current Science, 53:198–200.

Philipson L. (1983). Attachment of viruses to cell receptors and penetration of viruses into cells. *Textbook of Medical Virology*, 51–56. https://doi.org/10.1016/B978-0-407-00253-1.50012-8

Plait, P. 2024. Do Stars Outnumber the Sands of Earth's Beaches? https://www.scientificamerican.com/article/do-stars-outnumber-the-sands-of-earths-beaches/ Accessed July 24, 2025.

Parada, Ver' onica , Gerhard J. Herndl and Markus G. Weinbauer. 2006. Viral burst size of heterotrophic prokaryotes in aquatic systems. J. Mar. Biol. Ass. U.K. 86, 613–621

Ranasinghe, Nilakshi 2019. Literature study of virus size, burst size, latent period and genome size across different lytic eukaryotic and prokaryotic virus groups—an overview of traits and possible trade-offs. MSc Thesis. Department of biology, University of Bergen

Roughgarden, J., 2024. Lytic/lysogenic transition as a life-history switch. *Virus Evolution* 10(1), veae028, DOI: https://doi.org/10.1093/ve/veae028

Schwartz, M., 1976. The adsorption of coliphage lambda to its host: effect of variations in the surface density of receptor and in phage-receptor affinity. *Journal of molecular biology*, 103(3), pp.521–536

Silveira, Cynthia B., Antoni Luque and Forest Rohwer 2021. The landscape of lysogeny across microbial community density, diversity and energetics. Environmental Microbiology 23:4098–4111

Sobsey, M.D., Stauber, C.E., Casanova, L.M., Brown, J.M. and Elliott, M.A., 2008. Point of use household drinking water filtration: a practical, effective solution for providing sustained access to safe drinking water in the developing world. Environmental science & technology, 42(12), pp.4261-4267.

Srinivasiah, S., Bhavsar, J., Thapar, K., Liles, M., Schoenfeld, T., and Wommack, K. E. 2008. Phages across the biosphere: contrasts of viruses in soil and aquatic environments. Research in microbiology, 159(5):349–357.

Suttle, C. 2005 Viruses in the sea. Nature 437:356–361 https://doi.org/10.1038/nature04160

Suttle, C. 2007. Marine viruses—major players in the global ecosystem. Nat Rev Microbiol 5:801–12.

Townsend, E. M., Kelly, L., Muscatt, G., Box, J. D., Hargraves, N., Lilley, D., and Jameson, E. 2021. The human gut phageome: origins and roles in the human gut microbiome. Frontiers in cellular and infection microbiology, 11, 643214.

Van Charante, F., Holtappels, D., Blasdel, B. and Burrowes, B.H., 2021. Isolation of bacteriophages. Bacteriophages: biology, technology, therapy, pp.433–464.

Wang, I.N., Dykhuizen, D.E. and Slobodkin, L.B., 1996. The evolution of phage lysis timing. Evolutionary Ecology, 10, pp.545–558.

Wang, I.N., 2006. Lysis timing and bacteriophage fitness. *Genetics*, 172(1), pp.17–26.

Weinbauer, M. G. 2004. Ecology of prokaryotic viruses. FEMS microbiology reviews, 28(2):127–181

Weitz, J. S. 2016. Quantitative viral ecology: dynamics of viruses and their microbial hosts. Princeton University Press.

Whitman, W. B., Coleman, D. C., and Wiebe, W. J. 1998. Prokaryotes: the unseen majority. Proceedings of the National Academy of Sciences, 95(12):6578–6583.

Williamson, K. E., Fuhrmann, J. J., Wommack, K. E., and Radosevich, M. 2017. Viruses in soil ecosystems: an unknown quantity within an unexplored territory. Annual review of virology, 4(1):201–219

Wommack, K. E., and Colwell, R. R. 2000. Virioplankton: viruses in aquatic ecosystems. Microbiology and molecular biology reviews, 64(1):69–114.

Wommack, K.E., Williamson, K.E., Helton, R.R., Bench, S.R. and Winget, D.M., 2009. Methods for the isolation of viruses from environmental samples. Bacteriophages: methods and protocols, volume 1: isolation, characterization, and interactions, pp.3–14.